Advanced imaging in COPD: insights into pulmonary pathophysiology

Stephen Milne[1,2], Gregory G. King[1,3,4]

[1]The Woolcock Institute of Medical Research, Glebe, Sydney NSW 2037, Australia; [2]Northern Clinical School, University of Sydney, NSW 2006, Australia; [3]Northern and Central Clinical Schools, University of Sydney, NSW 2006, Australia; [4]Department of Respiratory Medicine, Royal North Shore Hospital, St Leonards, NSW 2065, Australia

Correspondence to: A/Prof. Gregory G. King. Woolcock Institute of Medical Research, PO Box M77, Camperdown NSW 2037, Australia. Email: ggk@woolcock.org.au.

Abstract: Chronic obstructive pulmonary disease (COPD) involves a complex interaction of structural and functional abnormalities. The two have long been studied in isolation. However, advanced imaging techniques allow us to simultaneously assess pathological processes and their physiological consequences. This review gives a comprehensive account of the various advanced imaging modalities used to study COPD, including computed tomography (CT), magnetic resonance imaging (MRI), and the nuclear medicine techniques positron emission tomography (PET) and single-photon emission computed tomography (SPECT). Some more recent developments in imaging technology, including micro-CT, synchrotron imaging, optical coherence tomography (OCT) and electrical impedance tomography (EIT), are also described. The authors identify the pathophysiological insights gained from these techniques, and speculate on the future role of advanced imaging in both clinical and research settings.

Keywords: Chronic obstructive pulmonary disease (COPD); respiratory physiology; medical imaging; pulmonary ventilation; respiratory function tests

Introduction

Chronic obstructive pulmonary disease (COPD) is a major cause of morbidity and mortality world-wide. Its impact is significant and increasing: COPD is predicted to be the 4th leading cause of death and the 7th leading contributor to the global burden of disease by 2030 (1). A better understanding of its pathophysiology, early detection and effective treatments is therefore imperative.

COPD involves at least two well-defined pathological features, namely parenchymal lung destruction (emphysema) and the loss or narrowing of airways (termed airways disease). The measureable physiological correlate of these changes is airflow obstruction, as indicated by a reduced spirometric ratio [forced expiratory volume in 1 second (FEV_1)/forced vital capacity (FVC)]. Until recently, these structural and physiological components have been studied in isolation, with inferences made about their relationship.

Advanced imaging techniques allow detailed anatomical and structural data to be acquired *in vivo*. Functional data can also be acquired, often in real-time, and co-registered with the anatomical images. In combination, these imaging data expose a remarkable degree of regional variation in lung function. Depending on the resolution of the images, information can be obtained down to the alveolar level (2). The different modalities vary greatly in terms of temporal and spatial resolution, and each has its own advantages and disadvantages.

In this review, we will describe advanced imaging modalities that are currently in use, either clinically or in a research setting, at varying stages of development. A large focus will be on their role in furthering our understanding of pathophysiology, clinical phenotyping and response to treatment. We will also speculate on the future place of

these techniques among the assortment of tools available to clinicians for managing COPD.

High-resolution computed tomography (HRCT)

X-ray computed tomography (CT) has been in commercial use since 1972 (3), and has been revolutionary in providing insight into pulmonary structure and function *in vivo*. The technology involves an X-ray beam source with a row of detectors positioned opposite—the source and detectors are assembled in a circular arrangement that rotates around the patient through 180 degrees. Measuring the attenuation of narrow X-ray beams as they pass through tissues of varying densities allows the construction of a 2-dimensional (x,y) axial 'slice' through the body. The digitised image slices are comprised of pixels with relative 'densities' [measured in Hounsfield Units (HU)] that are representative of the tissue density in that location. Early scanners used relatively thick, contiguous slices that were obtained along the cranio-caudal (z) axis as the patient was moved stepwise through the scanner.

High-resolution CT achieves its increased spatial resolution by the use of thinner detectors, which allows the effective thickness of the axial slices to be reduced, usually to around 1 mm. The physical size of the X-ray detectors is therefore one of the determinants of resolution, while scanning technique is the other and more dominant determinant of spatial resolution. The high-resolution technique traditionally involves axial or 2-dimensional scanning, i.e., subjects are stationary during a single tube rotation to acquire a single cross-sectional slice. Because of the increased time and radiation required to perform contiguous thin slices, the slices are typically separated along the z axis by an interval of around 10 mm, which minimises total radiation exposure but images only 10 percent of the lung. It is therefore suitable for imaging the lung parenchyma but not for detecting, for example, mass lesions.

These days, almost all CT scans are performed in 'helical' or 'spiral' mode, rather than the older axial technique. That is, the patient is moved continuously through the scanner during tube rotation, effectively producing a 'cork-screw' motion. In this way, 3-dimensional or volumetric data is obtained; the faster the patient is moved through the rotating tube (pitch), the faster the acquisition time and the lower the radiation exposure. However, this effectively produces greater blurring of the images and reduces spatial resolution. Hence imaging technique, including tube

current and voltage, once again has a large effect on spatial resolution.

Post-processing of the raw image data produces reconstructions in three orthogonal planes, which are most commonly displayed as axial images. Reconstruction also involves algorithms to produce images that are optimised for diagnostic viewing, such as 'high-resolution reconstruction algorithms'. These produce sharper but noisier images. Advances in CT technology have led to faster tube rotation, greater detector sensitivity and more rows of detectors – now up to 128 rows. This has greatly reduced acquisition time and reduced breath artifact; computer algorithms are able to correct for artifacts related to image inconsistency and motion (4). Axial slices of any thickness can be reconstructed, down to around 0.5 mm thickness (see *Figure 1*). However, at this level, spatial resolution is determined more by scanning technique (e.g., table speed) than by reconstructed slice thickness. There may therefore be no major advantage in such thin reconstructions. Modern post-processing techniques also allow true 3-dimensional reconstruction of the entire lung, airways and vasculature. Whether these are clinically useful is arguable.

Assessment of emphysema

HRCT is ideal for the detection and characterisation of emphysema (5). Moreover, it is very straightforward to use HRCT images to quantify the extent of emphysema. Older, standardised visual scoring systems to quantify emphysema (6) were subject to a high degree of inter- and intra-rater variability (7). More recent computer-automated quantification tools have removed the subjectivity of scoring (7). Emphysematous lung is represented by image voxels (the unit of a 3-dimensional image dataset) of density less than around –900 HU, which equates to a density of around 0.1 g/mL (water has a density of 1 g/mL). Identification of all voxels of density less than this threshold is a process commonly known as 'density masking', and the volume of the emphysematous lung can be calculated by multiplying the voxel numbers by the known volume of the voxels (8). A commonly used index is the percentage of low-attenuation areas (LAA%), which expresses the emphysema volume as a proportion of total lung volume measured by CT. The LAA% has been shown to correlate with FEV_1 (9-11), diffusing capacity for carbon monoxide (DLCO) (9), the frequency of COPD exacerbations (12), BODE index and quality of life scores (13). These relationships
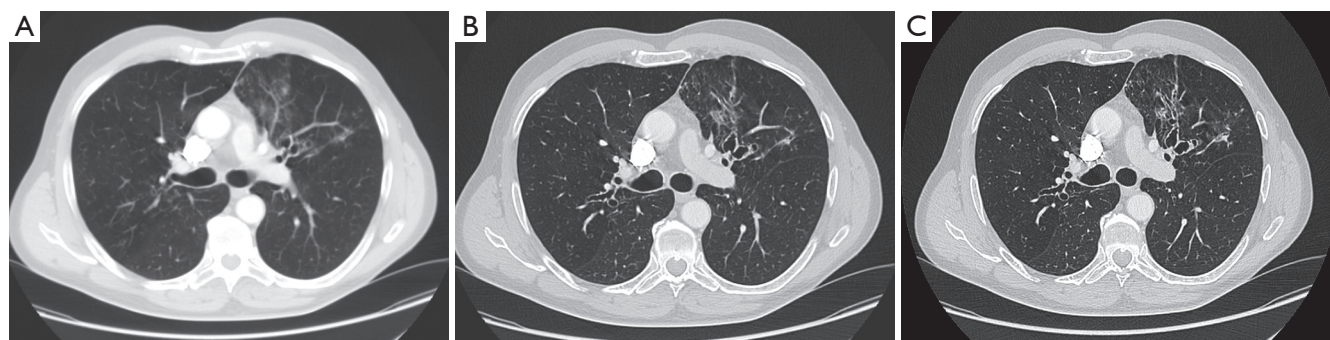
Figure 1 High-resolution CT scan of a 69-year-old man with allergic bronchopulmonary aspergillosis. Three axial reconstructions of (A) 6 mm, (B) 2.0 mm and (C) 0.625 mm thickness. Note the increasing spatial resolution with decreasing slice thickness. (Helical acquisition with the following settings to maximize spatial resolution: 120 kVp, 548 mAs, tube rotation time 0.5 s, collimator width 0.625 mm, pitch 1.375, voxel dimensions 0.76 mm × 0.76 mm × 0.625 mm).

confirm that the severity of emphysema is a determinant of the severity of airflow limitation as well as the clinical expression of disease.

A proposed clinical application of quantitative CT is in the longitudinal monitoring of emphysema progression. In the ECLIPSE study, which was a 3-year prospective, multi-centre observational study of COPD patients, emphysema progressed and became more extensive over the study period (14). The observations also confirmed that the extent of emphysema predicted the rate of decline of FEV_1 (15). Although it may be useful in identifying the so-called 'emphysematous phenotype', the ECLIPSE study also re-emphasised the marked clinical heterogeneity among COPD patients (16). More work is therefore needed to determine precisely how changes in CT emphysema over time translate into clinically important outcomes.

The LAA% gives an estimate of emphysema quantity, but not its distribution. The importance of emphysema distribution was demonstrated in the NETT (National Emphysema Treatment Trial) study of patients undergoing lung volume reduction surgery (LVRS). In this study, patients who had predominantly upper lobe emphysema (i.e., localised or heterogeneous emphysema, so-named because of the obvious differences in emphysematous and relatively preserved regions in the same lung) had improved survival following LVRS compared to the control group. In contrast, those in whom emphysema was not localised but rather spread out over a large proportion of the lung had poorer clinical outcomes (17).

In addition to this spatial heterogeneity, emphysematous lesions also exhibit so-called 'fractal geometry'. This is measured by identifying emphysematous clusters, i.e., a

discreet and isolated zone of emphysema. In COPD, there is a large number of small emphysematous lesions but only a small number of large lesions or cysts. Plotting a cumulative frequency of emphysematous lesion size in log-log space results in a linear relationship with a negative slope (18). The slope of that relationship is the 'fractal dimension', with a more negative slope indicating a more heterogeneous distribution of emphysema zone sizes. As an example of its clinical significance, Coxson *et al*. (19) showed that the fractal dimension derived from the pre-operative CT predicted the change in exercise capacity following LVRS. Although this complex CT assessment of emphysema appears to have some clinical significance, its potential role in routine clinical practice remains unclear.

Assessment of airways

Airways are also visible in HRCT image data, down to approximately generation 6 or 7. In COPD, changes in small airways (terminal and respiratory bronchioles) are considered to be the among the earliest signs of disease (20) and precede the development of emphysema (21). However, CT airway measurement is much more difficult than measurement of emphysema for a number of reasons. Firstly, airway branching is asymmetrical (in terms of length and calibre of bronchi) and hence 'functional' classification of individual airways cannot be made by simple counting of generations (22). Indeed, the small airways (0-2 mm in diameter) can be found anywhere between the 4th and 14th generations (22). Secondly, the measurable parameters of airway geometry (such as airway wall thickness and luminal area) vary greatly by anatomical location (23). Finally, since

the major site of airflow obstruction in COPD is in airways with dimensions less than 2 mm (20,21), the primary area of pathology is generally below the resolution of conventional HRCT.

Early attempts at quantitative analysis of visualised (generally large to medium sized) airways involved manual tracing of internal luminal area (Ai), outer area (Ao) and the calculation of wall area (Aw). Computer algorithms using a density mask have been used to automate this process, whereby circles surrounding the airway lumen are progressively 'eroded' based on density measures until the airway wall and lumen are identified (24). Another method known as the full-width-half-maximum method has been used to identify internal and external wall edges. This principle uses density analysis along radial 'spokes' from the centroid of the lumen, and identifies the wall edge as the point where density is half way between the local minimum and local maximum along each spoke (10). A well-documented problem is that CT measurement systematically over-estimates Aw and underestimates Ai, a feature that alters with airway angle and becomes more pronounced with decreasing airway calibre (24); mathematical corrections can be applied to overcome this error. Automated airway measurements have been validated for larger airways (down to the 6th generation) (25,26), but concerns regarding accuracy continue to limit their use.

Measurement of the small airways is even more problematic. Although large airway wall thickness correlates with symptoms (27) and lung function (10,25) in COPD, and may be predictive of small airway abnormalities (28), direct measurement of small airway geometry by CT has remained elusive. 'Air trapping' is an indirect HRCT measurement of small airway dysfunction, where lung lobules remain inflated due to airway obstruction and hence show a less-than-normal increase in attenuation during expiration, creating a mosaic pattern of attenuation. However, this phenomenon is observed to a degree even in healthy, non-smoking individuals without airflow obstruction (29,30). In COPD, this method is further complicated by the presence of emphysema, which itself shows low-attenuation during expiration (31). Although attempts at quantifying air trapping in the presence of COPD have been made (31,32), more validation studies are needed to determine the best method. For now, at least in the clinical setting, it seems that air trapping on CT will remain a more qualitative marker of small airways disease, and probably adds little to the diagnosis or monitoring in COPD.

Ventilation CT

Although anatomical information from CT is of value for diagnosis and assessment of disease severity, there is likely added benefit when it is combined with imaging-derived measurement of lung function. For example, the distribution of inhaled xenon (Xe) gas (which is radiopaque, and distributes into the airways and alveoli on inhalation) can be measured by its CT attenuation. The CT density of these Xe-containing airspaces increases linearly with Xe concentration (33). In this way, specific ventilation (i.e., ventilation per unit lung volume) can be measured and the regional distribution of ventilation explored. New dual-energy (i.e., two X-ray sources) CT allows both dynamic and static evaluation of regional ventilation, and simultaneous acquisition of anatomical and ventilation images (34). This eliminates the problems of serial scanning, such as differences in breath-hold volume affecting density, and spatial misregistration of the two scans (35). Dual-energy Xe gas ventilation scanning has been shown to reliably quantify both emphysema and airways disease (36).

Limitations of CT

In addition to problems with spatial resolution, CT has other important limitations. For example, there are minimal data regarding normal ranges for airway dimensions (37) and currently no consensus standards for validation and quality control of CT airway measurement—a prerequisite for high-quality, longitudinal studies. Perhaps the most important limitation of CT is the risk posed by ionising radiation, particularly with serial scanning (38). Quantitative measurements using current-generation detectors with low-dose protocols may be acceptable for certain applications (39) but the reduced signal-to-noise ratio poses an additional challenge when assessing small airways (40,41).

Ultra-high-resolution imaging

Like all diagnostic tools, imaging techniques need to be verified against a gold standard test. In the case of COPD, this would be histopathological evaluation of lung tissue. However, even as a gold standard, histopathology itself has problems: tissue changes from fixation, cutting and drying as the specimen is processed cause measurement error; the small size of specimens may introduce sampling error; and analysis is generally performed in two (or even single) dimensions, giving only estimates of the 3-dimensional
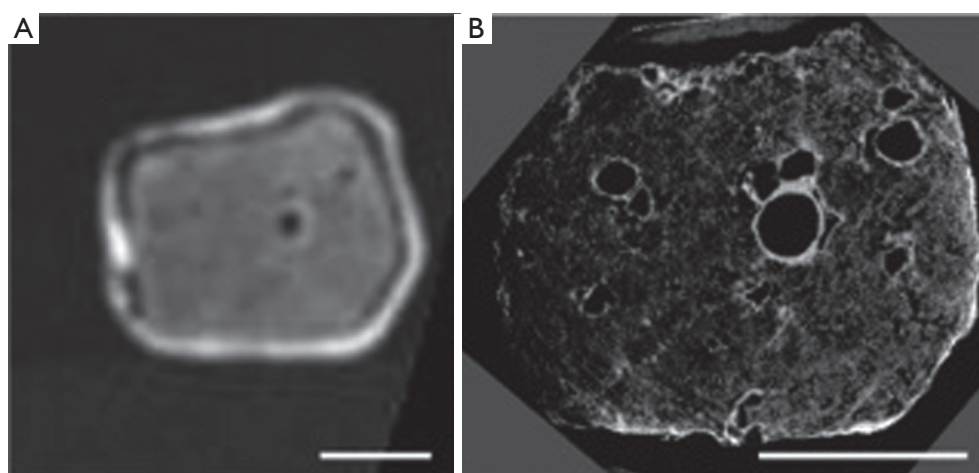
Figure 2 Micro-computed tomography (micro-CT) of a 2 cm pig lung cube. Lungs were inflation-fixed in formalin steam prior to scanning. (A) Cross-sectional high-resolution CT image and (B) corresponding micro-CT image of the same region of interest. Exquisite detail is seen with micro-CT. Scale bars =1 cm.

structure (42). The use of ultra-high-resolution imaging techniques is aimed at countering these problems.

Micro-computed tomography (micro-CT)

Micro-CT is similar to conventional CT in that it uses an X-ray source and detectors that are arranged around the study object. Like conventional CT, full volumetric data is captured. However, the source and detectors are brought much closer to the specimen, and the specimen itself is rotated while the X-ray source and detectors stay stationary. This allows exceptionally higher resolution (down to 1 µm per voxel), which is ideal for studying the lung microstructure including that of the small airways. The trade-offs are that only small specimens, i.e., excised tissue or small animals, can be imaged. Furthermore, the samples are exposed to high radiation doses that are damaging to living tissue.

Micro-CT was first used to image lung parenchyma by Watz *et al*. (43), who used a hot formalin vapour fixation technique and silver nitrate staining to provide the necessary contrast. This provided spectacular images of alveoli and terminal airways, and even allowed a "virtual bronchoscopy" through an alveolar duct (43). The technique has subsequently been validated against light microscopy in mouse lungs (44). It has also been used to generate gold-standard airway measurements from explanted lung to calibrate 3-dimensional airway measurements made by whole body HRCT (45). *Figure 2* demonstrates the

spectacular detail obtained using micro-CT of the lung. In COPD, micro-CT has been used to demonstrate the loss of terminal bronchioles in early-stage disease, which has been suggested to precede the microscopic emphysematous destruction of the alveoli (21).

Although living, *in vivo* human studies are precluded (due to both specimen size and the radiation dose), micro-CT has provided fascinating insights into the structural changes in COPD. The technology, in its currently form, will likely remain limited to research. It may play a future role in, for example, developing disease-modifying therapies in animal models.

Synchrotron imaging

This form of imaging utilises the properties of particle beams, e.g., electrons, in a particle accelerator. The particles are in continuous motion at near the speed of light, held in line by electromagnetic fields. When the particles are accelerated further they emit X-rays with a wide energy range, allowing a wide range of samples to be imaged, and a high photon flux, which allows fast acquisition times. The result is an image with resolution in the 1-10 µm range (46), which is ideally suited to studying the microstructure of fine tissues such as the lung.

The technique has been used to define the structure of both mouse (47) and human (48) lung acini *ex vivo*, as well as *in vivo* whole mouse lungs (49). The high temporal resolution also makes functional imaging possible,

including pulmonary acinar mechanics (50) and regional ventilation (51,52). In COPD mouse models, it has been used to identify early emphysematous changes (53,54). While the anatomical detail is impressive, synchrotron imaging is yet to provide significant functional information on human lungs, being hampered by the limitations of specimen size (necessitating excised tissue or small animals only), radiation damage to tissues, and the need for a particle accelerator.

Nuclear medicine imaging

Unlike CT imaging methods, which are based on the relative absorbance of radiation transmitted through the tissues from an external source, nuclear medicine techniques utilise tracers that emit radiation and are introduced into the organs. This has been used to image a variety of body tissues and organs, including bone, the heart and the brain. Nuclear medicine scanners are in routine clinical use for the diagnosis and staging of malignancy. They have also long been used for the diagnosis of pulmonary embolism (PE)—this involves intravenous injection of radioisotopes to the pulmonary vasculature and inhalation to the peripheral airspaces, thus giving functional images of ventilation and perfusion.

Positron emission tomography (PET)

PET is a 3-dimensional nuclear imaging technique, which utilises radioisotopes that emit positrons as they decay. A positron is a sub-atomic particle found in the nucleus, with the same molecular weight as an electron. As the positron makes its way out of the nucleus, it encounters a free electron—these two oppositely-charged particles combine and 'annihilate' each other. In the process, two identical beams of gamma-radiation are emitted at 180 degrees to each other—beams detected at or very near the same time are considered to be 'coincident' i.e., from the same source. The location of the source particle can therefore be determined geometrically from coincident beams, being located on a straight line between the two detectors. However, this localisation is affected by beam scatter, the presence of random coincidences, and by attenuation as the beams travel through tissues of different densities. Corrections for this image noise can be made during image processing, which includes the use of a tissue density map i.e., a CT scan. Many scanners incorporate multi-detector CT (PET-CT) so that, in addition to providing a tissue density map for attenuation correction, organ function

can be superimposed onto the CT images. This image co-registration has an obvious application in oncology for localisation of active tumour cells for targeted treatment.

The most commonly used PET radioisotope is fluorine-18, which has a half-life of approximately 110 minutes. This isotope is attached to fluorodeoxyglucose (FDG, a glucose analogue) to form the radiotracer 18F-FDG. The radiotracer is taken up by metabolically active tissue—a property used to identify cancerous tissue in the lungs and surrounding structures. In COPD, 18F-FDG has been used to demonstrate an increase in neutrophilic inflammation in the lungs compared to controls and to those with alpha-1 antitrypsin deficiency-associated emphysema (55). This provides interesting insights into COPD pathophysiology and is a non-invasive, *in vivo* measurement. However, it is also potentially useful in studies of new therapies targeting neutrophils, given their role in the pathogenesis and pathophysiology of COPD (56).

Regional ventilation can also be measured by PET using the PET isotope nitrogen-13 (13NN) gas dissolved in saline. A peripheral venous injection of this tracer enters the lung via the pulmonary arterial circulation. Due to its low tissue solubility, the 13NN then rapidly diffuses across the alveolar membrane. An initial breath-hold during injection allows the 13NN to enter the lung in direct proportion to blood flow, which allows measurement of regional perfusion. Regional ventilation can subsequently be measured by the decrease in 13NN activity over time as the subject breathes, clearing the 13NN in direct proportion to ventilation (57). Combining this information thus produces the regional distribution of lung ventilation/perfusion ratios (V/Q). Quantification of regional V/Q by PET has been shown to correlate closely with global measures of gas exchange such as arterial partial pressure of oxygen (PaO$_2$) (58). Using this 13NN technique in COPD, Brudin and colleagues (59) reported that high V/Q tended to be more common in subjects with an emphysematous phenotype, whereas low V/Q was more common in those with a small airways disease phenotype. This is consistent with the archetypal concept of 'pink puffers' and 'blue bloaters'.

While much of the focus in COPD is on airways disease and changes in regional ventilation, there has been an increasing focus on the role of the pulmonary vasculature in this disease. Vidal Melo *et al*. (60) found that regional heterogeneity in Q was increased in patients with mild COPD compared to healthy controls, in a manner that was independent of changes in regional tissue density. This very interesting finding suggests that regional changes in

pulmonary blood flow, perhaps due to inflammation, may precede lung parenchymal changes in COPD. This may have utility as a biomarker for early disease.

One limitation of PET, with its short half-life radioisotopes, is the need for a cyclotron and radiopharmaceutical formulation often on-site. Additionally, for repeated studies, the radioisotope has to decay enough to avoid signal contamination. Adjustments following a 'baseline' scan prior to repeat administration help overcome this problem, however rapid, repeat testing is generally not possible. The spatial resolution of PET does not allow imaging of individual gas exchange units, although it is probably sufficient to separate physiologically meaningful differences in regional ventilation.

In spite of these limitations, and its relatively recent inception, PET may have a significant future in the study of COPD. The recent findings regarding regional distribution of blood flow may provide insight into the role of vascular remodeling, especially with regard to longitudinal changes and therapies targeted at this process.

Single-photon emission computed tomography (SPECT)

SPECT is similar to PET in that a radiotracer is introduced to the body, and the radiation it emits is detected externally. However there are several key differences. SPECT radioisotopes emit a single gamma-beam as they decay, as opposed to the two gamma beams emitted simultaneously from PET isotopes. This results in a lower radiation exposure to the patient, at the expense of an increased acquisition time per image. Increased scanning time may decrease resolution due to movement artifact, although there have been attempts to overcome this with breath hold/respiratory gating (61). The spatial resolution of SPECT is less than that of PET, however it is more widely available, and SPECT radiotracers are easier and cheaper to manufacture. SPECT has been a major advance in nuclear imaging for suspected PE (62), as opposed to the traditional planar lung scintigraphy. The more recent appearance of SPECT-CT fusion has helped overcome a lot of the resolution and anatomical registration problems, and can provide true 3D assessment of regional lung function (63,64).

In addition to its diagnostic role for PE, SPECT can give us insights into pulmonary physiology, both with respect to ventilation and perfusion. Perfusion scanning is generally performed using 99m-technecium labeled macro-aggregated albumin (^{99m}Tc-MAA), which lodges in the pulmonary circulation after peripheral injection. Ventilation scanning requires inhalation of gaseous radioisotopes or radiolabeled particulate aerosols. A true gas distributes throughout the whole lung, and differences in its regional distribution reflect differences in regional ventilation. Dynamic SPECT could therefore potentially give information on the time course of ventilation in different lung regions. Both ^{81m}Kr (65) and ^{133}Xe (66) have been used to demonstrate ventilation heterogeneity in COPD.

Unlike true gases, particulate aerosol tracers are 'deposited' in the lung and have the advantage that imaging can be performed without the tracer continuously redistributing. Also, aerosols will not distribute by collateral ventilation between lung units, which is increased in COPD compared with healthy lungs. However, aerosol particles of a diameter 0.5-1 µm are 1,000 times larger than gas molecules and are therefore transported by convective ventilation only (67). The distribution of radioaerosols therefore neglects diffusive ventilation, which is the predominant mode of gas transport within acini beyond the terminal bronchiole (68). In COPD, airway narrowing and emphysematous destruction likely brings the convection-diffusion front more centrally so that a larger volume of the lung ventilates by diffusion compared with healthy lungs. Therefore, the interpretation of inhaled radioaerosols distributions in COPD should take these physiological changes into account (69).

A commonly used aerosol tracer is 99m-technecium-labelled diethylene triamine pentaacetic acid (^{99m}Tc-DTPA). The generated particle size is around 1 µm but this increases on entry into the airways due to agglomeration. These larger particles deposit onto large airways, particularly at airway branch points, causing 'hot-spots' on the ventilation image (70). Technegas is a ^{99m}Tc-labelled, aerosolised ultra-fine carbon particle of approximately 200 nm diameter. It is used routinely in Australia (where it was invented) and other countries in V/Q scanning for the diagnosis of PE. Due to its small particle size, the distribution of Technegas approximates that of a true gas (71), even in the presence of severe airflow obstruction (72) (*Figure 3*). Technegas deposits more homogenously, and is less susceptible to central airway deposition or movement after inhalation, than ^{99m}Tc-DTPA (73).

Regional V/Q ratios are heterogeneous in COPD due to the variable effects of inflammation and tissue destruction on lung parenchyma, small airways and blood vessels. Jogi *et al*. (74) reported significant relationships between SPECT-derived V/Q ratios and both airflow obstruction measured by spirometry and emphysema severity on CT. In
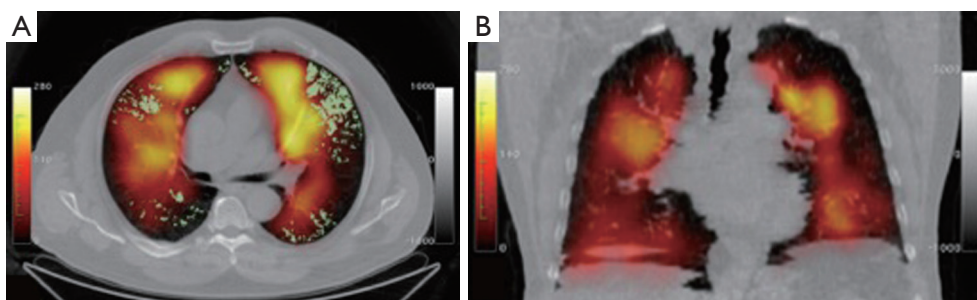
Figure 3 Technegas ventilation SPECT/CT fusion images of a 68-year-old man with moderately severe COPD. (A) Axial dimension, with well-ventilated areas (bright yellow), less ventilated areas (red) and non-ventilated areas (black). Green indicates emphysema determined by a CT density mask, with pixel density less than –910 HU. Note that poorly ventilated areas tend to correspond to areas of emphysema. Some non-ventilated areas are not associated with emphysema, suggesting airway obstruction without macroscopic parenchymal destruction in these areas; (B) coronal reconstruction of ventilation map.

patients with COPD, Suga *et al.* (75) found that automated, quantitative analysis of V/Q distribution by SPECT was more sensitive at detecting early emphysema than the corresponding CT density mask. The standard deviation of the V/Q profile (i.e., dispersion of V/Q ratios) could differentiate the GOLD spirometric classes of severity, and also correlated well with the measured alveolar-arterial oxygen gradient (A-aDO2), a global measure of V/Q inequality (75).

There have been a number of intervention studies in COPD patients using nuclear scintigraphy techniques, including SPECT, to predict and measure clinical success. For example, SPECT imaging has been shown to predict post-operative lung function following surgery for lung cancer. Sudoh *et al.* (76) demonstrated that perfusion SPECT/CT was as accurate as the segment-counting technique (77) but was less affected by the presence of severe emphysema (76). In emphysematous patients undergoing LVRS, Inmai and colleagues (78) found that LVRS improved ventilation distribution as measured by Technegas SPECT, not only in the surgical field but also in the contralateral lung. Recently, Argula *et al.* (79) performed a retrospective analysis of data from the VENT endobronchial valve study (80) to investigate the effects of baseline lobar perfusion on outcomes following endobronchial valve placement. In this analysis, target lobe perfusion was quantified from ^{99m}Tc-MAA perfusion images taken prior to stent insertion. The patients were dichotomised as 'high' or 'low' baseline lobar perfusion. Post-procedure, the low perfusion group were found to have a significantly greater increased in 6-minute walk distance at 6 months, which was independent of the degree

of emphysematous destruction in that lobe. The authors postulate that the redistribution of blood flow seen in the 'high' baseline perfusion group may explain their poorer exercise performance (79). This study used planar scintigraphy, and it is possible that similar studies using the more sophisticated SPECT/CT may shed further light on this interesting finding. To date, there are no published studies using SPECT ventilation imaging to assess the effects of treatments aimed at improving the ventilation patterns in COPD, including bronchodilators, inhaled corticosteroid therapy, bronchial stents or intrapulmonary thermal treatment.

In summary, there have been many technical advances in SPECT imaging of lung ventilation and perfusion. There are potentially many research questions in COPD to which SPECT imaging could be applied, particularly because of its relative wide availability in large centres. Future studies will inform eventual clinical applications in COPD. Although PET ventilation imaging could eventually be preferred over SPECT, the current availability and cost of PET may limit its use.

Magnetic resonance imaging (MRI)

MRI has the advantage of not requiring ionising radiation. Its usefulness for lung imaging has traditionally been limited by technical factors and, consequently, there has been much less MRI lung imaging in research and clinical practice compared with the modalities already discussed. The technique employs large magnetic fields, which alter the behavior of individual atoms. Conventional MRI utilises the nuclear spin properties of hydrogen atoms, found in

abundance in water. In their natural state, hydrogen ions (or protons) spin on an axis in random orientations. The application of a strong and uniform magnetic field causes them to align parallel or anti-parallel to the field. When the magnetic field is switched off, the spinning protons return to their natural state and in the process release a burst of radiofrequency energy. It is this energy that is detected by the MRI scanner, and is used to construct the image. MRI has excellent anatomical resolution in tissues of high water content, such as the brain. However the lung, being mostly air, has a low density of hydrogen ions, meaning low signal intensity and poor signal-to-noise ratio. Conventional proton MRI images of the lung therefore have low contrast and contain little meaningful information. Additionally, being comprised of air-filled alveolar sacs, the lung has millions of air-tissue interfaces. Each of these causes decay of the radiofrequency signal as it travels through the lung, known as 'susceptibility artifact', which contributes to poor signal intensity (81). Such inherent limitations have left the lung relatively unexplored by MRI. However, the large potential for MRI imaging of the lung has been recognised for decades (82) and thus many attempts have been made to overcome these barriers.

Inhaled noble gas MRI

Inhaled noble gases have been used to overcome the aforementioned limitations (83). Unlike particulate aerosols, gases undergo 'self-diffusion' by random Brownian motion, where the gas molecules continually move further apart until stopped by a physical boundary. The speed and direction of movement is determined by the physical properties of the gas, and the likelihood of colliding with a neighbouring gas particle i.e., the local concentration of the gas. An example of a noble gas ventilation agent is hyperpolarised helium-3 which, unlike air, is highly excitable by a magnetic field and thus provides excellent MRI contrast. It diffuses freely in air at a rate of 0.88 cm^2/s, which means that, over a timecourse of 2 ms, an individual molecule will travel 0.59 mm. Given that the typical acinar size is 0.3 mm, the diffusive movement of a molecule of ^{3}He in an acinus will be limited by the alveolar boundaries within the 2 ms timeframe—that is, its diffusion will be 'restricted' from 0.88 to 0.2 cm^2/s. The restricted gas molecule movement is measurable by MRI, and is known as the 'apparent diffusion coefficient (ADC)'. A high ADC indicates that the alveolar walls are further apart, i.e., there is alveolar destruction or acinar expansion, which is an early sign of emphysema (84).

The technique has been validated against histological specimens (2). It is increased in smokers who still have a normal FEV$_1$, suggest that alveolar expansion and early emphysema are present even without clinical manifestation of disease (85). The ADC also correlates very closely with standard lung function measures including FEV$_1$/FVC ratio, TLC and RV (85). In more advanced disease, the mean ADC correlates strongly with FEV$_1$ (86) and DLCO (87), in fact more strongly than HRCT measures of emphysema (86,87).

From a functional perspective, ventilation can also be assessed using the properties of inhaled noble gases. Inhalation of the hyperpolarised gas distributes reasonably homogeneously in healthy young adults, but is heterogeneous in otherwise healthy elderly subjects (81). Regions of absent MRI signal, which indicate non- or poorly-ventilated lung units, have been shown to correlate with emphysema that is detectable by CT or the ADC (88). Ventilation defects may also be observed even in the absence of anatomically gross emphysema visible by CT (89,90). In this case, small airways disease, mucous plugging or a combination of both small airways diseases and microscopic emphysema are possible explanations for absent ventilation. This suggests that, like PET and SPECT, functional disturbances measured by MRI may be more sensitive markers of early abnormalities in COPD, compared with anatomical imaging by HRCT.

The ability of hyperpolarised ^{129}Xe to diffuse across the alveolar membrane into the circulation allows gas exchange to be measured. There is a large chemical shift of ^{129}Xe between the gas compartment, the dissolved (tissue and plasma) compartment and the red blood cells (91). By detecting the change in resonance frequency between these compartments, measures of the alveolar membrane thickness (91) and blood uptake (92) can be made. This technique has been used to demonstrate the influence of posture on regional perfusion heterogeneity (93) as well as ventilation heterogeneity (94) in COPD.

Oxygen-enhanced MRI

Although the use of hyperpolarised noble gases has greatly advanced the use of MRI for lung imaging, these gases are expensive to use, requiring specialised laser polarising equipment and dedicated detectors. ^{3}He in particular is in limited and restrictive supply. There is therefore a need for simpler and less expensive contrast agents. Oxygen was suggested as a MRI contrast agent by Edelman (95) over 15 years ago as a way of overcoming the inherent

limitations of conventional proton MRI and avoiding the problems of hyperpolarised gases. Ohno and Hatabu (96) have written a detailed review of the theory and application of oxygen-enhanced MRI. In basic terms, molecular oxygen is weakly paramagnetic and, in the concentrations found in air and in blood, provides little MR signal. The inhalation of 100% oxygen produces a high concentration of oxygen in alveolar tissue and in blood, where is it predominantly dissolved in plasma. The result is an increase in the signal intensity, which then allows visualisation of the pulmonary parenchyma. The difference between room-air and oxygen-enhanced images represents ventilation to that area. Edelman's original publication (95) clearly showed ventilation defects in a patient with emphysema. Ohno and colleagues (97) showed that oxygen-enhanced MRI was as good as CT at quantifying pulmonary emphysema across a wide range of severities, and correlated reasonably well with FEV_1 and DLCO. Recent work in subjects with COPD has shown increased heterogeneity of V/Q distribution measured by oxygen-enhanced MRI even in those without CT-defined emphysema (98), which varies with the severity of COPD (99).

The advantages of oxygen-enhanced MRI (OE-MRI) are that it is a simple, low-cost and safe alternative to hyperpolarised gas MRI. One of the limitations is that the gas itself is not directly visualised, but rather the tissue and blood, so that OE-MRI is only an indirect measure of ventilation. Another limitation is that the absorption of oxygen by circulating blood removes it from the lung unit, meaning there would inevitably be a difference between the wash-in and wash-out phases if they were measured. Additionally, the administration of 100% oxygen to patients, particularly those with advanced COPD, may alter the fundamental pulmonary physiology that we are attempting to measure (96).

In summary, MRI is increasing our current understanding of regional ventilation in COPD, whilst overcoming the limitations of ionising radiation associated with other functional imaging modalities. Cost and availability of the gases, polarisers and research scanning time will likely remain major constraints. Therefore, OE-MRI may be more practical in terms of clinical application. More studies are needed to build on the limited treatment (100,101) and longitudinal (102) data available to date.

Emerging imaging modalities

Optical coherence tomography (OCT)

OCT has emerged from the field of interventional pulmonology. It involves the measurement of lung structure from an endobronchial approach. Analogous to B-mode ultrasound but utilising light waves rather than sound waves, OCT involves the insertion of a near-infrared optical probe into the airway, with a sensor to detect back-scattered and reflected light waves. A detailed description of the physics of OCT is present in Huang's seminal review of the topic (103). OCT images have sufficient resolution to distinguish between different tissue types within the airways, i.e., mucosa, sub-mucosa, lamina propria, cartilage, airway smooth muscle and alveoli. This ability of OCT can therefore potentially identify malignant tissue at the time of bronchoscopy, where the structural components of tissues are altered in their organisation, content and reflective properties (104).

Although there are few studies in subjects with COPD, OCT is ideally placed to measure the anatomical properties of small airways, being limited only by the physical reach of the probe and by the need for repeated measurements in different areas to obtain representative sampling. Miniaturised probes can be introduced down to the level of the terminal bronchiole (105,106). Coxson and colleagues demonstrated an excellent correlation between airway dimension measured by OCT and by CT (107). OCT may give more accurate measurement of airways size since, in this study, CT-measured dimensions tended to be larger than the OCT measurements. Furthermore, OCT airway dimensions measured at the 5th generation bronchi showed a strong negative correlation with the subject's FEV_1, and had greater discriminatory power for airflow obstruction than CT measurements (107). There was also an increase in %wall area and an increase the density of subepithelial structures in subjects with a lower FEV_1 (107). Kirby et al. (108) reported a strong negative correlation between airway wall area and FEV_1 in males COPD subjects but not in females, which is an interesting observation that may be relevant to the observed differences in disease behavior between the sexes (109,110).

OCT shows promise as a very useful tool for relating structural and functional changes in COPD in vivo. There are very important advantages of high resolution, the ability to measure small airways and the lack of ionising radiation, but it is nevertheless an invasive procedure requiring at least conscious sedation. The potentially important and novel information on small airways means that it will likely be increasingly used in research and clinical practice as the technology improves and becomes more accessible.

Electrical impedance tomography (EIT)

As its name suggests, EIT measures differences in impedance to the flow of an electrical current through different tissues. A typical setup involves a set of surface electrodes, usually 16 to 32, positioned around a body structure. Through a pair of electrodes (the 'drive pair') a small current is applied. The potential difference between each pair of adjacent electrodes is then recorded, and hence the resistivity or impedance at that location can be determined. The process is repeated with each pair of electrodes acting as the drive pair, and a spatial map of resistivity is developed. This technique is ideally suited to pulmonary monitoring for several reasons. Firstly, the lungs, being filled with air, have naturally high impedance and are subject to large changes in volume during respiration. This gives a relatively large 'swing' in impedance that can be used to monitor breathing patterns and interventions. The change in electrical lung impedance is proportional to the change in gas content, which has been validated against other imaging modalities (111-113). Secondly, a decrease in impedance from initially high values could be used to detect focal consolidation/collapse or more diffuse changes in, for example, acute respiratory distress syndrome (ARDS). Thirdly, the short acquisition time provides enough temporal resolution for real-time monitoring of the lungs over long periods, as opposed to quasi-dynamic imaging of ventilation CT or nuclear medicine. Finally, being small and portable, EIT can be used in a variety of physical settings.

Even though the potential clinical utility of EIT respiratory monitoring has been recognised for many years (114), the pulmonary application of EIT has so far been largely limited to the intensive care setting. For example, EIT has been used to develop protective ventilation strategies by optimising positive end-expiratory pressure (PEEP) to minimise regional hyperinflation and collapse (115). In a case report of a patient with COPD undergoing mechanical ventilation, Mauri et al. (116) could optimise ventilator settings to overcome intrinsic PEEP and decrease gas trapping measured with OCT. More recently, the technique has been used to explore other obstructive airways diseases. Zhao and colleagues (117) showed that, in patients with cystic fibrosis, regional airway obstruction measured by OCT correlated with a CT composite index of bronchiectasis severity, mucous plugging, parenchymal opacity and hyperinflation in the same lung region.

The most detailed physiological study using EIT in subjects with COPD was recently published by Vogt et al. (118). EIT was used to measure the regional distribution of tidal volume, inspiratory vital capacity and FEV_1 during a forced expiratory manoeuvre. Ventilation heterogeneity between regions was quantified as the coefficient of variation. COPD subjects showed greater ventilation heterogeneity than either young or older healthy subjects. Importantly, the measurements were able to discriminate between healthy and COPD subjects even during quiet tidal breathing.

EIT therefore represents an exciting new technique for assessing regional ventilation in COPD. It is a simple, portable, radiation-free, real-time measurement that would be well suited to dynamic physiological studies. More work is needed to determine its role in, for example, the early detection of disease and for treatment/intervention studies.

Conclusions

Our understanding of the pathophysiological mechanisms in COPD is increasing with the new era of imaging tools that are available. There is a greater recognition of the complexity of lung mechanics and regional ventilatory abnormalities in this clinically heterogeneous disease, and advanced imaging techniques are at the forefront of this investigation. As older techniques are refined, and new techniques are developed, the information we gain from advanced imaging in COPD is likely to expand exponentially. The major limitation of ionising radiation exposure is being overcome by advances in technology, which minimise radiation dose while increasing image quality. These modalities are likely to become increasingly important in drug design and delivery, and offer the chance to monitor the impact of such therapies over time. Ultimately, the aims of COPD research should be directed towards modifying the natural history of the disease. We believe the role of advanced imaging techniques in detecting disease in its earliest stage is paramount, as this is the stage at which potentially disease-modifying interventions are likely to have the greatest impact.

Acknowledgements

References

1. Mathers CD, Loncar D. Projections of global mortality and burden of disease from 2002 to 2030. PLoS Med 2006;3:e442.
2. Woods JC, Choong CK, Yablonskiy DA, et al. Hyperpolarized 3He diffusion MRI and histology in pulmonary emphysema. Magn Reson Med 2006;56:1293-300.
3. Pan X, Siewerdsen J, La Riviere PJ, et al. Anniversary Paper: Development of x-ray computed tomography: The role of Medical Physics and AAPM from the 1970s to present. Med Phys 2008;35:3728-39.
4. Crawford CR, King KF. Computed tomography scanning with simultaneous patient translation. Med Phys 1990;17:967-82.
5. Bergin CJ, Muller NL, Miller RR. CT in the qualitative assessment of emphysema. J Thorac Imaging 1986;1:94-103.
6. Goddard PR, Nicholson EM, Laszlo G, et al. Computed tomography in pulmonary emphysema. Clin Radiol 1982;33:379-87.
7. Sakai N, Mishima M, Nishimura K, et al. An automated method to assess the distribution of low attenuation areas on chest CT scans in chronic pulmonary emphysema patients. Chest 1994;106:1319-25.
8. Müller NL, Staples CA, Miller RR, et al. "Density mask". An objective method to quantitate emphysema using computed tomography. Chest 1988;94:782-7.
9. Cerveri I, Dore R, Corsico A, et al. Assessment of emphysema in COPD: a functional and radiologic study. Chest 2004;125:1714-8.
10. Nakano Y, Muro S, Sakai H, et al. Computed tomographic measurements of airway dimensions and emphysema in smokers. Correlation with lung function. Am J Respir Crit Care Med 2000;162:1102-8.
11. Timmins SC, Diba C, Farrow CE, et al. The relationship between airflow obstruction, emphysema extent, and small airways function in COPD. Chest 2012;142:312-9.
12. Han MK, Kazerooni EA, Lynch DA, et al. Chronic obstructive pulmonary disease exacerbations in the COPDGene study: associated radiologic phenotypes. Radiology 2011;261:274-82.
13. Martinez CH, Chen YH, Westgate PM, et al. Relationship between quantitative CT metrics and health status and BODE in chronic obstructive pulmonary disease. Thorax 2012;67:399-406.
14. Coxson HO, Dirksen A, Edwards LD, et al. The presence and progression of emphysema in COPD as determined by CT scanning and biomarker expression: a prospective analysis from the ECLIPSE study. Lancet Respir Med 2013;1:129-36.
15. Vestbo J, Edwards LD, Scanlon PD, et al. Changes in forced expiratory volume in 1 second over time in COPD. N Engl J Med 2011;365:1184-92.
16. Agusti A, Calverley PM, Celli B, et al. Characterisation of COPD heterogeneity in the ECLIPSE cohort. Respir Res 2010;11:122.
17. Fishman A, Martinez F, Naunheim K, et al. A randomized trial comparing lung-volume-reduction surgery with medical therapy for severe emphysema. N Engl J Med 2003;348:2059-73.
18. Mishima M, Hirai T, Itoh H, et al. Complexity of terminal airspace geometry assessed by lung computed tomography in normal subjects and patients with chronic obstructive pulmonary disease. Proc Natl Acad Sci U S A 1999;96:8829-34.
19. Coxson HO, Whittall KP, Nakano Y, et al. Selection of patients for lung volume reduction surgery using a power law analysis of the computed tomographic scan. Thorax 2003;58:510-4.
20. Hogg JC, Macklem PT, Thurlbeck W. Site and nature of airway obstruction in chronic obstructive lung disease. N Engl J Med 1968;278:1355-60.
21. McDonough JE, Yuan R, Suzuki M, et al. Small-airway obstruction and emphysema in chronic obstructive pulmonary disease. N Engl J Med 2011;365:1567-75.
22. Hogg JC. Pathophysiology of airflow limitation in chronic obstructive pulmonary disease. Lancet 2004;364:709-21.
23. Kuwano K, Bosken CH, Paré PD, et al. Small airways dimensions in asthma and in chronic obstructive pulmonary disease. Am Rev Respir Dis 1993;148:1220-5.
24. King GG, Muller NL, Whittall KP, et al. An analysis algorithm for measuring airway lumen and wall areas from high-resolution computed tomographic data. Am J Respir Crit Care Med 2000;161:574-80.
25. Hasegawa M, Nasuhara Y, Onodera Y, et al. Airflow limitation and airway dimensions in chronic obstructive pulmonary disease. Am J Respir Crit Care Med 2006;173:1309-15.
26. Orlandi I, Moroni C, Camiciottoli G, et al. Chronic Obstructive Pulmonary Disease: Thin-Section CT Measurement of Airway Wall Thickness and Lung Attenuation. Radiology 2005;234:604-10.
27. Grydeland TB, Dirksen A, Coxson HO, et al. Quantitative computed tomography measures of emphysema and airway wall thickness are related to respiratory symptoms. Am J

Respir Crit Care Med 2010;181:353-9.

28. Nakano Y, Wong JC, de Jong PA, et al. The Prediction of Small Airway Dimensions Using Computed Tomography. Am J Respir Crit Care Med 2005;171:142-6.

29. Tanaka N, Matsumoto T, Miura G, et al. Air Trapping at CT: High Prevalence in Asymptomatic Subjects with Normal Pulmonary Function 1. Radiology 2003;227:776-85.

30. Hashimoto M, Tate E, Watarai J, et al. Air trapping on computed tomography images of healthy individuals: effects of respiration and body mass index. Clin Radiol 2006;61:883-7.

31. Matsuoka S, Kurihara Y, Yagihashi K, et al. Quantitative assessment of air trapping in chronic obstructive pulmonary disease using inspiratory and expiratory volumetric MDCT. AJR Am J Roentgenol 2008;190:762-9.

32. Hersh CP, Washko GR, Estépar RS, et al. Paired inspiratory-expiratory chest CT scans to assess for small airways disease in COPD. Respir Res 2013;14:42.

33. Murphy DM, Nicewicz JT, Zabbatino SM, et al. Local pulmonary ventilation using nonradioactive xenon-enhanced ultrafast computed tomography. Chest 1989;96:799-804.

34. Chae EJ, Seo JB, Goo HW, et al. Xenon Ventilation CT with a Dual-Energy Technique of Dual-Source CT: Initial Experience 1. Radiology 2008;248:615-24.

35. Chae EJ, Seo JB, Lee J, et al. Xenon ventilation imaging using dual-energy computed tomography in asthmatics: initial experience. Invest Radiol 2010;45:354-61.

36. Park E-A, Goo JM, Park SJ, et al. Chronic Obstructive Pulmonary Disease: Quantitative and Visual Ventilation Pattern Analysis at Xenon Ventilation CT Performed by Using a Dual-Energy Technique 1. Radiology 2010;256:985-97.

37. Montaudon M, Lederlin M, Reich S, et al. Bronchial measurements in patients with asthma: comparison of quantitative thin-section CT findings with those in healthy subjects and correlation with pathologic findings 1. Radiology 2009;253:844-53.

38. Sodickson A, Baeyens PF, Andriole KP, et al. Recurrent CT, Cumulative Radiation Exposure, and Associated Radiation-induced Cancer Risks from CT of Adults. Radiology 2009;251:175-84.

39. Tschirren J, Hoffman EA, McLennan G, et al. Intrathoracic airway trees: segmentation and airway morphology analysis from low-dose CT scans. IEEE Trans Med Imaging 2005;24:1529-39.

40. Schilham AM, van Ginneken B, Gietema H, et al. Local noise weighted filtering for emphysema scoring of low-dose CT images. IEEE Trans Med Imaging 2006;25:451-63.

41. Yuan R, Mayo JR, Hogg JC, et al. The effects of radiation dose and CT manufacturer on measurements of lung densitometry. Chest 2007;132:617-23.

42. Ochs M, Mühlfeld C. Quantitative microscopy of the lung: a problem-based approach. Part 1: basic principles of lung stereology. Am J Physiol Lung Cell Mol Physiol 2013;305:L15-L22.

43. Watz H, Breithecker A, Rau WS, et al. Micro-CT of the Human Lung: Imaging of Alveoli and Virtual Endoscopy of an Alveolar Duct in a Normal Lung and in a Lung with Centrilobular Emphysema—Initial Observations 1. Radiology 2005;236:1053-8.

44. Vasilescu DM, Klinge C, Knudsen L, et al. Stereological assessment of mouse lung parenchyma via nondestructive, multiscale micro-CT imaging validated by light microscopic histology. J Appl Physiol 2013;114:716-24.

45. Dame Carroll JR, Chandra A, Jones AS, et al. Airway dimensions measured from micro-computed tomography and high-resolution computed tomography. Eur Respir J 2006;28:712-20.

46. Westneat MW, Socha JJ, Lee WK. Advances in Biological Structure, Function, and Physiology Using Synchrotron X-Ray Imaging. Annu Rev Physiol 2008;70:119-42.

47. Yong HS, Kang EY, Kim YK, et al. Phase contrast microradiography of mouse lung using synchrotron X-ray: correlation with optical microscopy. Yonsei Med J 2009;50:422-6.

48. Litzlbauer HD, Korbel K, Kline TL, et al. Synchrotron-based micro-CT imaging of the human lung acinus. Anat Rec (Hoboken) 2010;293:1607-14.

49. Parsons DW, Morgan K, Donnelley M, et al. High-resolution visualization of airspace structures in intact mice via synchrotron phase-contrast X-ray imaging (PCXI). J Anat 2008;213:217-27.

50. Sera T, Yokota H, Tanaka G, et al. Murine pulmonary acinar mechanics during quasi-static inflation using synchrotron refraction-enhanced computed tomography. J Appl Physiol 2013;115:219-28.

51. Dubsky S, Hooper SB, Siu KK, et al. Synchrotron-based dynamic computed tomography of tissue motion for regional lung function measurement. J R Soc Interface 2012;9:2213-24.

52. Kitchen MJ, Lewis RA, Morgan MJ, et al. Dynamic measures of regional lung air volume using phase contrast x-ray imaging. Phys Med Biol 2008;53:6065-77.

53. Schleede S, Meinel FG, Bech M, et al. Emphysema diagnosis using X-ray dark-field imaging at a laser-driven

compact synchrotron light source. Proc Natl Acad Sci U S A 2012;109:17880-5.

54. Yaroshenko A, Meinel FG, Bech M, et al. Pulmonary Emphysema Diagnosis with a Preclinical Small-Animal X-ray Dark-Field Scatter-Contrast Scanner. Radiology 2013;269:427-33.

55. Subramanian DR, Jenkins L, Edgar R, et al. Assessment of pulmonary neutrophilic inflammation in emphysema by quantitative positron emission tomography. Am J Respir Crit Care Med 2012;186:1125-32.

56. Jones HA, Soler N. Quantification of Pulmonary Inflammation by Positron Emission Tomography in Chronic Obstructive Pulmonary Disease: A New Horizon in the Era of Biomarkers? Am J Respir Crit Care Med 2012;186:1071-3.

57. Harris RS, Winkler T, Tgavalekos N, et al. Regional pulmonary perfusion, inflation, and ventilation defects in bronchoconstricted patients with asthma. Am J Respir Crit Care Med 2006;174:245.

58. Vidal Melo MF, Layfield D, Harris RS, et al. Quantification of regional ventilation-perfusion ratios with PET. J Nucl Med 2003;44:1982-91.

59. Brudin LH, Rhodes CG, Valind SO, et al. Regional structure-function correlations in chronic obstructive lung disease measured with positron emission tomography. Thorax 1992;47:914-21.

60. Vidal Melo MF, Winkler T, Harris RS, et al. Spatial heterogeneity of lung perfusion assessed with (13)N PET as a vascular biomarker in chronic obstructive pulmonary disease. J Nucl Med 2010;51:57-65.

61. Suga K, Kawakami Y, Iwanaga H, et al. Assessment of anatomic relation between pulmonary perfusion and morphology in pulmonary emphysema with breath-hold SPECT-CT fusion images. Ann Nucl Med 2008;22:339-47.

62. Reinartz P, Wildberger JE, Schaefer W, et al. Tomographic imaging in the diagnosis of pulmonary embolism: A comparison between V/Q lung scintigraphy in SPECT technique and multislice spiral CT. J Nucl Med 2004;45:1501-8.

63. Suga K. Pulmonary function-morphologic relationships assessed by SPECT-CT fusion images. Ann Nucl Med 2012;26:298-310.

64. Harris B, Bailey DL, Chicco P, et al. Objective analysis of whole lung and lobar ventilation/perfusion relationships in pulmonary embolism. Clin Physiol Funct Imaging 2008;28:14-26.

65. Stavngaard T, Søgaard LV, Mortensen J, et al. Hyperpolarised 3He MRI and 81mKr SPECT in chronic obstructive pulmonary disease. Eur J Nucl Med Mol Imaging 2005;32:448-57.

66. Suga K, Nishigauchi K, Kume N, et al. Dynamic pulmonary SPECT of xenon-133 gas washout. J Nucl Med 1996;37:807-14.

67. Santolicandro A, Ruschi S, Fornai E, et al. Imaging of ventilation in chronic obstructive pulmonary disease. J Thorac Imaging 1986;1:36-53.

68. Crawford AB, Makowska M, Paiva M, et al. Convection- and diffusion-dependent ventilation maldistribution in normal subjects. J Appl Physiol (1985) 1985;59:838-46.

69. King GG, Harris B, Mahadev S. V/Q SPECT: utility for investigation of pulmonary physiology. Semin Nucl Med 2010;40:467-73.

70. Cabahug CJ, McPeck M, Palmer LB, et al. Utility of technetium-99m-DTPA in determining regional ventilation. J Nucl Med 1996;37:239-44.

71. Amis TC, Crawford AB, Davison A, et al. Distribution of inhaled 99mtechnetium labelled ultrafine carbon particle aerosol (Technegas) in human lungs. Eur Respir J 1990;3:679-85.

72. Crawford AB, Davison A, Amis TC, et al. Intrapulmonary distribution of 99mtechnetium labelled ultrafine carbon aerosol (Technegas) in severe airflow obstruction. Eur Respir J 1990;3:686-92.

73. Jögi J, Jonson B, Ekberg M, et al. Ventilation-perfusion SPECT with 99mTc-DTPA versus Technegas: a head-to-head study in obstructive and nonobstructive disease. J Nucl Med 2010;51:735-41.

74. Jögi J, Ekberg M, Jonson B, et al. Ventilation/perfusion SPECT in chronic obstructive pulmonary disease: an evaluation by reference to symptoms, spirometric lung function and emphysema, as assessed with HRCT. Eur J Nucl Med Mol Imaging 2011;38:1344-52.

75. Suga K, Kawakami Y, Koike H, et al. Lung ventilation–perfusion imbalance in pulmonary emphysema: assessment with automated V/Q quotient SPECT. Ann Nucl Med 2010;24:269-77.

76. Sudoh M, Ueda K, Kaneda Y, et al. Breath-hold single-photon emission tomography and computed tomography for predicting residual pulmonary function in patients with lung cancer. J Thorac Cardiovasc Surg 2006;131:994-1001.

77. Nakahara K, Monden Y, Ohno K, et al. A method for predicting postoperative lung function and its relation to postoperative complications in patients with lung cancer. Ann Thorac Surg 1985;39:260-5.

78. Inmai T, Sasaki Y, Shinkai T, et al. Clinical evaluation of

99mTc-Technegas SPECT in thoracoscopic lung volume reduction surgery in patients with pulmonary emphysema. Ann Nucl Med 2000;14:263-9.

79. Argula RG, Strange C, Ramakrishnan V, et al. Baseline regional perfusion impacts exercise response to endobronchial valve therapy in advanced pulmonary emphysema. Chest 2013;144:1578-86.

80. Sciurba FC, Ernst A, Herth FJ, et al. A Randomized Study of Endobronchial Valves for Advanced Emphysema. N Engl J Med 2010;363:1233-44.

81. Washko GR, Parraga G, Coxson HO. Quantitative pulmonary imaging using computed tomography and magnetic resonance imaging. Respirology 2012;17:432-44.

82. Mayo JR, MacKay A, Müller NL. MR imaging of the lungs: value of short TE spin-echo pulse sequences. AJR Am J Roentgenol 1992;159:951-6.

83. Albert MS, Cates GD, Driehuys B, et al. Biological magnetic resonance imaging using laser-polarized 129Xe. Nature 1994;370:199-201.

84. Hartroft WS. The Microscopic Diagnosis of Pulmonary Emphysema. Am J Pathol 1945;21:889-903.

85. Quirk JD, Lutey BA, Gierada DS, et al. In vivo detection of acinar microstructural changes in early emphysema with (3)He lung morphometry. Radiology 2011;260:866-74.

86. Ley S, Zaporozhan J, Morbach A, et al. Functional evaluation of emphysema using diffusion-weighted 3Helium-magnetic resonance imaging, high-resolution computed tomography, and lung function tests. Invest Radiol 2004;39:427-34.

87. van Beek EJ, Dahmen AM, Stavngaard T, et al. Hyperpolarised 3He MRI versus HRCT in COPD and normal volunteers: PHIL trial. Eur Respir J 2009;34:1311-21.

88. Kirby M, Svenningsen S, Kanhere N, et al. Pulmonary ventilation visualized using hyperpolarized helium-3 and xenon-129 magnetic resonance imaging: differences in COPD and relationship to emphysema. J Appl Physiol 2013;114:707-15.

89. Mathew L, Kirby M, Etemad-Rezai R, et al. Hyperpolarized 3He magnetic resonance imaging: Preliminary evaluation of phenotyping potential in chronic obstructive pulmonary disease. Eur J Radiol 2011;79:140-6.

90. Parraga G, Ouriadov A, Evans A, et al. Hyperpolarized 3He ventilation defects and apparent diffusion coefficients in chronic obstructive pulmonary disease: preliminary results at 3.0 Tesla. Invest Radiol 2007;42:384-91.

91. Cleveland ZI, Cofer GP, Metz G, et al. Hyperpolarized Xe

MR imaging of alveolar gas uptake in humans. PLoS ONE 2010;5:e12192.

92. Mugler JP, 3rd, Altes TA, Ruset IC, et al. Simultaneous magnetic resonance imaging of ventilation distribution and gas uptake in the human lung using hyperpolarized xenon-129. Proc Natl Acad Sci U S A 2010;107:21707-12.

93. Kaushik SS, Freeman MS, Cleveland ZI, et al. Probing the regional distribution of pulmonary gas exchange through single-breath gas- and dissolved-phase 129Xe MR imaging. J Appl Physiol 2013;115:850-60.

94. Dregely I, Mugler JP, 3rd, Ruset IC, et al. Hyperpolarized Xenon-129 gas-exchange imaging of lung microstructure: first case studies in subjects with obstructive lung disease. J Magn Reson Imaging 2011;33:1052-62.

95. Edelman RR, Hatabu H, Tadamura E, et al. Noninvasive assessment of regional ventilation in the human lung using oxygen–enhanced magnetic resonance imaging. Nat Med 1996;2:1236-9.

96. Ohno Y, Hatabu H. Basics concepts and clinical applications of oxygen-enhanced MR imaging. Eur J Radiol 2007;64:320-8.

97. Ohno Y, Iwasawa T, Seo JB, et al. Oxygen-enhanced magnetic resonance imaging versus computed tomography: multicenter study for clinical stage classification of smoking-related chronic obstructive pulmonary disease. Am J Respir Crit Care Med 2008;177:1095-102.

98. Zhang W, Hubbard P, Bondesson E, et al. Ventilation-perfusion mismatch in COPD with or without emphysema: Comparison of structural CT and functional OE-MRI. Eur Respir J 2011;38:1882.

99. Hubbard PL, Parker GJ, Singh D, et al. Novel ventilation-perfusion ratio measurements in COPD using MRI. Eur Respir J 2011;38:1880.

100. Kirby M, Heydarian M, Wheatley A, et al. Evaluating bronchodilator effects in chronic obstructive pulmonary disease using diffusion-weighted hyperpolarized helium-3 magnetic resonance imaging. J Appl Physiol (1985) 2012;112:651-7.

101. Kirby M, Mathew L, Heydarian M, et al. Chronic Obstructive Pulmonary Disease: Quantification of Bronchodilator Effects by Using Hyperpolarized He MR Imaging. Radiology 2011;261:283-92.

102. Kirby M, Mathew L, Wheatley A, et al. Chronic Obstructive Pulmonary Disease: Longitudinal Hyperpolarized 3He MR Imaging. Radiology 2010;256:280-9.

103. Huang D, Swanson EA, Lin CP, et al. Optical coherence tomography. Science 1991;254:1178-81.

104. Tsuboi M, Hayashi A, Ikeda N, et al. Optical coherence tomography in the diagnosis of bronchial lesions. Lung Cancer 2005;49:387-94.
105. Coxson HO, Lam S. Quantitative assessment of the airway wall using computed tomography and optical coherence tomography. Proc Am Thorac Soc 2009;6:439-43.
106. McLaughlin RA, Yang X, Quirk BC, et al. Static and dynamic imaging of alveoli using optical coherence tomography needle probes. J Appl Physiol 2012;113:967-74.
107. Coxson HO, Quiney B, Sin DD, et al. Airway wall thickness assessed using computed tomography and optical coherence tomography. Am J Respir Crit Care Med 2008;177:1201.
108. Kirby M, Zhang W, Laratta PK, et al. Sex differences in chronic obstructive pulmonary disease evaluated using optical coherence tomography. Society of Photo-Optical Instrumentation Engineers (SPIE) Conference Series, 2014.
109. Sørheim IC, Johannessen A, Gulsvik A, et al. Gender differences in COPD: are women more susceptible to smoking effects than men? Thorax 2010;65:480-5.
110. Dransfield MT, Davis JJ, Gerald LB, et al. Racial and gender differences in susceptibility to tobacco smoke among patients with chronic obstructive pulmonary disease. Respir Med 2006;100:1110-6.
111. Hinz J, Neumann P, Dudykevych T, et al. Regional ventilation by electrical impedance tomography: A comparison with ventilation scintigraphy in pigs. Chest 2003;124:314-22.
112. Richard JC, Pouzot C, Gros A, et al. Electrical impedance tomography compared to positron emission tomography for the measurement of regional lung ventilation: an experimental study. Crit Care 2009;13:R82.
113. Victorino JA, Borges JB, Okamoto VN, et al. Imbalances in regional lung ventilation: a validation study on electrical impedance tomography. Am J Respir Crit Care Med 2004;169:791-800.
114. Brown BH, Barber DC, Seagar AD. Applied potential tomography: possible clinical applications. Clin Phys Physiol Meas 1985;6:109-21.
115. Costa EL, Borges JB, Melo A, et al. Bedside estimation of recruitable alveolar collapse and hyperdistension by electrical impedance tomography. Intensive Care Med 2009;35:1132-7.
116. Mauri T, Bellani G, Salerno D, et al. Regional Distribution of Air Trapping in Chronic Obstructive Pulmonary Disease. Am J Respir Crit Care Med 2013;188:1466-7.
117. Zhao Z, Müller-Lisse U, Frerichs I, et al. Regional airway obstruction in cystic fibrosis determined by electrical impedance tomography in comparison with high resolution CT. Physiol Meas 2013;34:N107-14.
118. Vogt B, Pulletz S, Elke G, et al. Spatial and temporal heterogeneity of regional lung ventilation determined by electrical impedance tomography during pulmonary function testing. J Appl Physiol 2012;113:1154-61.